Translational Oncology
www.transonc.com

Volume 13 Number 2 February 2020 pp. 372–382 372

Epigenetic Regulation of RIP3 Suppresses Necroptosis and Increases Resistance to Chemotherapy in NonSmall Cell Lung Cancer

Qiong Wang[*,†,1], Peipei Wang[‡,1], Li Zhang[§,1], Mathewos Tessema[*], Lang Bai[*,‖], Xiuling Xu[*], Qin Li[†], Xuelian Zheng[†], Bryanna Saxton[*], Wenshu Chen[*], Randy Willink[*], Zhiping Li[¶], Lin Zhang[†], Steven A. Belinsky[*], Xia Wang[†,‡], Bin Zhou[†] and Yong Lin[*]

[*]Molecular Biology and Lung Cancer Program, Lovelace Respiratory Research Institute, 2425 Ridgecrest DR. SE, Albuquerque, NM, 87108, USA; [†]Laboratory of Molecular and Translational Medicine, Key Laboratory of Birth Defects and Related Diseases of Women and Children (Sichuan University) of Ministry of Education, Department of Obstetrics and Gynecology, West China Second University Hospital, Sichuan University, Chengdu 610041, China; [‡]Department of Immunology, West China School of Basic Medical Sciences & Forensic Medicine, Sichuan University, Chengdu, Sichuan, 610041, China; [§]Laboratory of Pathology, West China Hospital, Sichuan University, Chengdu, 610041, China; [‖]Center of Infectious Diseases, West China Hospital, Sichuan University, Chengdu, 610041, China; [¶]Department of Abdominal Oncology, West China Hospital, Sichuan University, Chengdu, 610041, China

Abstract

INTRODUCTION: The efficacy of chemotherapeutic agents in killing cancer cells is mainly attributed to the induction of apoptosis. However, the tremendous efforts on enhancing apoptosis-related mechanisms have only moderately improved lung cancer chemotherapy, suggesting that other cell death mechanisms such as necroptosis could be involved. In this study, we investigated the role of the necroptosis pathway in the responsiveness of nonsmall cell lung cancer (NSCLC) to chemotherapy. **METHODS:** In vitro cell culture and in vivo xenograft tumor therapy models and clinical sample studies are combined in studying the role of necroptosis in chemotherapy and mechanism of necroptosis suppression involving RIP3 expression regulation. **RESULTS:** While chemotherapeutic drugs were able to induce necroptotic cell death, this pathway was suppressed in lung cancer cells at least partly through downregulation of RIP3 expression. Ectopic RIP3 expression significantly sensitized lung cancer cells to the cytotoxicity of anticancer drugs such as cisplatin, etoposide, vincristine, and adriamycin. In addition, RIP3 suppression was associated with RIP3 promoter methylation, and demethylation partly restored RIP3 expression and increased chemotherapeutic-induced necroptotic cell death. In a xenograft tumor therapy model, ectopic RIP3 expression significantly sensitized anticancer activity of cisplatin in vivo. Furthermore, lower RIP3 expression was associated with worse chemotherapy response in NSCLC patients.

Address all correspondence to: Bin Zhou, PhD, Laboratory of Molecular and Translational Medicine, West China Second University Hospital, Sichuan University, Chengdu 610041, China. E-mail: zhoubin630@scu.edu.cn or Xia Wang, PhD, Department of Immunology, West China School of Basic Medical Sciences & Forensic Medicine, Sichuan University, Chengdu, Sichuan 610041, China. E-mail: xiawang@scu.edu.cn or Yong Lin, MD, PhD, Molecular Biology and Lung Cancer Program, Lovelace Respiratory Research Institute, 2425 Ridgecrest Dr., SE, Albuquerque, NM 87108, USA. E-mail: ylin@lrri.org

[1]These authored contributed equally to this work.

Received 22 November 2019; Accepted 25 November 2019

1936-5233/19
https://doi.org/10.1016/j.tranon.2019.11.011

CONCLUSION: Our results indicate that the necroptosis pathway is suppressed in lung cancer through RIP3 promoter methylation, and reactivating this pathway should be exploited for improving lung cancer chemotherapy.

Translational Oncology (2020) 13, 372–382

Introduction

Lung cancer is the leading cause of cancer-related death worldwide, and development of effective therapy is critical for reducing mortality caused by this malignant disease [1]. Nonsmall cell lung cancer (NSCLC) accounts for 80−85% of all lung cancer cases and is responsible for the majority of lung cancer mortality [1,2]. Although most patients with advanced lung cancer rely on chemotherapy, the efficacy of it is often significantly undermined due to inherent or acquired chemoresistance. While different molecular pathways are involved in promoting the efficacy of chemotherapeutics, activation of cell death pathways play a direct role for the anticancer mechanisms of chemotherapy [3]. Thus, evading programmed cell death pathways is not only one of the hallmarks of cancer but also contributes to chemoresistance and is the main cause of therapy failure [4]. Chemotherapeutics kill cancer cells mainly through apoptosis activation, and innate and acquired apoptosis resistance substantially contributes to chemoresistance [5]. Extensive research efforts have been devoted toward elucidating the mechanisms for overcoming apoptosis resistance. However, this has only achieved a moderate improvement in the effectiveness of anticancer chemotherapy [6]. Other cell death pathways are also involved in anticancer drug-induced cancer cytotoxicity [7]. Thus, elucidating novel mechanisms underlying the role of these cell death pathways in chemoresistance could be valuable for improving survival of lung cancer patients.

Recent studies suggest that necroptosis, receptor-interacting protein 3 (RIP3, also known as RIPK3)-dependent programmed necrosis [8,9], can be activated by chemotherapeutics [10−12]. Necroptosis can be activated in certain cell types when apoptosis pathways are blocked. However, under certain circumstances, necroptosis could also be the predominant cell death pathway in the presence of competent apoptosis pathways [13]. Thus, necroptosis can be either a dominant or an alternative cell death mechanism for chemotherapy-induced cytotoxicity. Many stimuli induce necroptosis through the formation of a complex named necrosome (also called ripoptosome), consisting of RIP3, RIP1, FADD, and caspase 8 [14]. When caspase 8 is suppressed, RIP1 mediates RIP3 phosphorylation and activation, which in turn activates MLKL, resulting in reactive oxygen species (ROS) production and necroptotic cell death [15]. Suppressing NF-κB through RIP1 deubiquitilation by cIAPs triggers necroptosis [16]. Interestingly, certain anticancer therapeutics such as etoposide induces necrosome formation and necroptosis [11]. Therefore, sensitizing necroptosis may be used for anticancer therapy in treating cancers that are apoptosis resistant [7], and determining the role of necroptosis in cancer cells could significantly impact therapeutic strategies to improve overall response and patient survival [17].

RIP3 is a ubiquitously expressed protein that has an N-terminal kinase domain, a RIP homotypic interaction motif (RHIM) and a unique C-terminal domain [18]. Although early reports suggested a role for RIP3 in NF-κB and apoptosis signaling, RIP3 knockout failed to reveal any alteration in the NF-κB signaling or apoptosis triggered by TNFα or other stimuli [19], suggesting that RIP3 is not a mediator for apoptosis or the NF-κB pathway. Recent studies have revealed that necroptosis is the major type of cell death mediated by RIP3. RIP3 knockout mice are resistant to virus-induced tissue necrosis and necrosis-mediated inflammation in an acute pancreatitis mouse model [20−22]. Consistently, RIP3 knockout or knockdown cells are refractory to necroptosis induced by different stimuli [20−23].

In this study, we investigated the role of necroptosis in lung cancer cells' response to chemotherapy and the mechanisms underlying chemoresistance involving RIP3 inactivation. The results show that while chemotherapeutic drugs induce necroptotic cell death, this cell death pathway is suppressed at least partly due to epigenetic suppression of RIP3 expression in lung cancer, and suggest a novel mechanism for improving anticancer chemotherapy. Exploiting the RIP3-mediated necroptosis pathway may open an important avenue for improving chemotherapy efficacy against lung cancer.

Materials and Methods

Reagents

Cisplatin (cDDP, 479306), etoposide (E1383), vincristine (V8388), and adriamycin (doxorubicin, D1515) were purchased from Sigma (St. Louis, MO). Anti-RIP3 (B-2, sc-374639, used for Western blot), -β-actin (A1978), and -GAPDH (sc-32233) were from Santa Cruz Biotechnology (Santa Cruz, CA). Anti-MLKL (clone 3H1, MABC604) and -phospho-MLKL (Ser358, 17-10400) were from Millipore Sigma (Burlington, MA). Anti-cyclophilin A (#2175) and -active caspase-3 (#9664) were from Cell Signaling Technology (Danvers, MA). Anti-poly (ADP-ribose) polymerase (PARP, ALX-210-302) and zVAD-FMK (ALX-260-020) were from Enzo Life Sciences Inc. (Ann Arbor, MI). Anti-GFP was from Clontech (632380, Mountain View, CA). Necrosulfonamide (NSA, ab143839) was from Abcam (Cambridge, MA). Anti-RIP3 (505431, used for IHC) was from Zen-Bioscience (Chengdu, Sichuan, China). Human NSCLC tissue array (LC1006) was from US Biomax (Derwood, MD). In Situ Cell Death Detection Kit-TMR red was from Roche Applied Science (12156792910, Mannheim, Germany).

Human Lung Cancer Tissue Samples

Human lung cancer tissue section samples for immunohistochemistry (IHC) assays were obtained from the tissue bank of West China Hospital, Sichuan University (Chengdu, China), and pathologically diagnosed by two expert pathologists. All patients provided informed consent. This research was approved by the Institutional Review Board of Sichuan University (approval notice No. 2017-114). Frozen

tumor tissues from 16 NSCLC patients were obtained from tumor banks at the University of New Mexico. Distant normal lung tissue (DNLT) obtained from the resected lobe was available for a subset of these cases. All samples were obtained with written informed consent from patients, and the study was approved by the institute's Ethics Committee.

Cell Culture and Transfections

NSCLC cell lines A549, H1568, H1299, H460, H23, H2009, H2023, H1689, HCC4006, Calu-3, and Calu-6 were from American Type Culture Collection (ATCC, Manassas, VA), authenticated by short tandem repeat (STR) DNA profiling (Genetica Cell Line Testing, Burlington, NC), and maintained in RPMI-1640 with 2 mM of glutamine and antibiotics penicillin (100 U/ml) and streptomycin (100 μg/ml) (Thermo Fisher Scientific, Waltham, MA) supplemented with 10% fetal bovine serum (Atlanta Biologicals, Flowery Branch, GA). All cells were grown under standard incubator conditions at 37 °C, with 5% CO_2. Immortalized human bronchial epithelial cells, HBEC-2 and -13, were generously provided by Drs. Shay and Minna, Southwestern Medical Center, Dallas, TX [24].The HBEC cell lines were maintained in Keratinocyte serum free medium (K-SFM) (Invitrogen), supplemented with 5 μg/L of human recombinant EGF and 50 mg/L of bovine pituitary extract in plates coated with FNC coating mix (Athena ES).

For stable transfection of pEGFP-N1-RIP3 expressing plasmid [21], a gift of Dr. Chan FK, University of Massachusetts Medical School, was transfected to cells using Fugene HD (Promega, Madison, WI) and stably transfected cells were selected with 500 μg/ml of G418 (Sigma). Positive clones were identified by Western blot and expanded and maintained in medium with 200 μg/ml of G418. The OmicsLink MLKL shRNA Expression Clones (GeneCopoeia, Rockville, MD, USA) were transfected using Fugene HD and selected with 4 μg/ml of puromycin. The MLKL shRNA sequences are: MLKL shRNA-1 (HSH004664-7-LVRH1GP(OS397199): 5′-gcattgcaatagtgaggcaga-3’; MLKL shRNA-2 (HSH004664-8-LVRH1GP(OS397200): 5′-ggtaactcaaggctaccaagt-3’. For transient knockdown studies, siGENOME MLKL (M-005326-00-0005) and RIP3 (M-003534-01-0005) siRNAs from Thermo Scientific (Waltham, MA) were used. The cells were seeded in 12-well plates at about 60−70% confluence, transfected with the specific siRNA using INTE RFERin siRNA transfection reagent (Polyplus-transfection) according to manufacturer's instructions.

Western Blot

Cells were collected and lysed, and equal amounts of proteins were separated by 10 or 12% SDS-polyacrylamide gels and then transferred to PVDF membranes. The membranes were incubated with the primary and secondary antibodies sequentially; the proteins on the membranes were detected by enhanced chemiluminescence (ECL, Millipore). The intensity of the individual bands was quantified by densitometry (ImageJ) and normalized to the corresponding loading control bands. Fold changes were calculated with the control taken as 1 [25,26].

Cell Viability Assays

Cell viability was assessed using a 3-(4,5-dimethylthiazolyl-2-)-2,5-diphenyltetrazolium bromide (MTT) cell proliferation assay as described previously [27]. Briefly, the cells were seeded in 48-well plates at 50-60% confluence overnight, and then treated as indicated in the associated figure legends. After treatment, cells were washed twice with PBS and were incubated in MTT solution for 2−3 hours. The percentage of viable cells was calculated using the following formula: Cell viability (%) = (Absorbance of treated sample/Absorbance of control) × 100. For long-term cell survival assay, the cells in 24-well plates at a density of 1×10^4 cells/well were treated as in the figure legends for 48 hours, washed with PBS, and maintained in RPMI-1640 medium with 10% of FBS for 10 days. Cell colonies were stained with methylene blue and photographed.

DNA Methylation Analysis

DNA extraction, modification, and methylation analysis using Combined Bisulfite Restriction Analysis (COBRA) were performed as described [28]. The primers used for COBRA were: RIPK3 meth2F: 5′-AGGTTTTTTGGTATTTTTTAGTTTGATG-3’; RIPK3 meth2R: 5′-TCAAACCCCAAAACACAATAACTCC-3’. Amplification conditions: 94 °C 1min, 64 °C 1 min, 72 °C 1min, for 40 cycles. The PCR products were digested with *Taq I* or *Bst I,* separated in 1% agarose gels, and visualized. For methylation-specific PCR (MSP), the primers used were RIPK3 BSM1: 5′-GGTATGTC-GATCGTAGTTTTC-3’; RIPK3 BSM2:5′- CCACTAACC-GACCGTACCG-3’. Amplification conditions: 94 °C 30 s, 64 °C 30 s and 72 °C 30 s for 38 cycles. Quantitative methylation data for RIP3 including its promoter CpG islands was obtained from our recent HumanMethylation450 beadchip (HM450K) analysis of lung tumor−normal pairs and cell lines [29,30]. Treatment of NSCLC cell lines with the DNA methylation inhibitor 5-aza-2′-deoxycytidine (DAC, 1 μM every 24 hours for 96 hours) or the histone deacetylase inhibitor Trichostatin A (TSA, 300 nM for 18 hours) just before harvesting for RNA or protein analysis was performed as described [28].

Quantitative Reverse Transcription-Polymerase Chain Reaction (qRT-PCR)

Total RNA was extracted from each sample using TRIzol Reagent (Life technology). Two micrograms of RNA were used as a template for cDNA synthesis with a reverse transcription kit (Promega, Madison, WI). An equal volume of cDNA product was subjected to PCR analysis. TaqMan assays for human RIP3 (Hs01011177_g1*) and the endogenous control housekeeping gene β-actin (4310881E) both from Applied Biosystems were used in a multiplex PCR to quantify the relative expression of RIP3. Samples were run at least twice in duplicate and RIP3 expression relative to the endogenous control (ΔCT) and the reference control samples (ΔΔCT) was calculated in fold-change as described [31].

Xenograft Tumor Chemotherapy Study

BALB/c nude mice (6 weeks old, male and female) were obtained from the Animal Center of Sichuan University (Chengdu, China). All procedures involving animals and their care were conducted in accordance with the guidelines of the Institutional Animal Care and Use Committee of Sichuan University. A549 cells with ectopic EGFP-RIP3 expression by stable transfection (RIP3 group) or the EGFP-vector control (negative control group, NC group) were resuspended in 0.05 ml of PBS (1.5×10^6) and mixed with 0.05 ml of matrigel (BD bioscience, Franklin Lakes, NJ) and then injected

subcutaneously into the flanks of nude mice. After palpable tumors had developed, the mice were randomly divided into two subgroups and administrated with either PBS or cisplatin (4 mg/kg) by i.p. injection once a week. The tumor length and width were measured with a clipper, and the tumor volume (V) was calculated using the following formula: $V = \text{length} \times \text{width}^2/2$. At the end of experiment, animals were euthanized. The tumors were excised and weighed. The antitumor effect of cisplatin for RIP3 group and NC group was expressed as the tumor inhibitory rate: [(mean tumor weight of PBS group - tumor weights of the cisplatin-treated group)/mean tumor weight of PBS group] × 100%.

TUNEL Assay and Immunofluorescent Staining

Following the cell death detection guidelines [32–34], in situ TUNEL assay combined with immunofluorescent staining of active caspase-3 were carried out in paraffin-embedded tumor tissue sections. TUNEL assay was based on labeling of DNA strand breaks by using the in situ cell death detection kit (12156792910, Roche Applied Science, Mannheim, Germany) according to the manufacturer's instructions. Briefly, after dewaxation, rehydration, protease treatment, and permeabilization, the tumor tissue sections were incubated with the terminal deoxynucleotidyl transferase labeling reaction mixture for 60 min at 37 °C. The slides were then incubated with antiactive caspase-3 antibody (Cell Signaling Technology, Danvers, MA, #9664) overnight at 4 °C followed by goat antirabbit IgG (Alexa Fluor 647) (ab150083, Abcam) for 60 min at 37 °C. Nucleus was stained with DAPI. The sections were evaluated under a laser scanning confocal microscope using an excitation wavelength of 543 nm for TUNEL staining, 633 nm for active caspase-3 staining, and 488 nm for DAPI staining. The TUNEL-positive cells showed red fluorescence. The active caspase-3 positive cells showed yellow fluorescence. The dead cells showing positive for TUNEL but negative for active caspase 3 were regarded as necroptotic whereas those positive for both TUNEL and active caspase 3 were regarded as apoptotic [32–34].

Statistics

All quantitative data are expressed as mean ± SD. Statistical significance was examined by two-way analysis of variance (ANOVA). $P < 0.05$ was considered statistically significant.

Results

Chemotherapeutics Induce Necroptosis in NSCLC Cells

We examined if necroptosis can be activated in NSCLC cells when exposed to cisplatin (cDDP), a first-line chemotherapeutic agent for lung cancer. As expected, cisplatin treatment induced cell death and

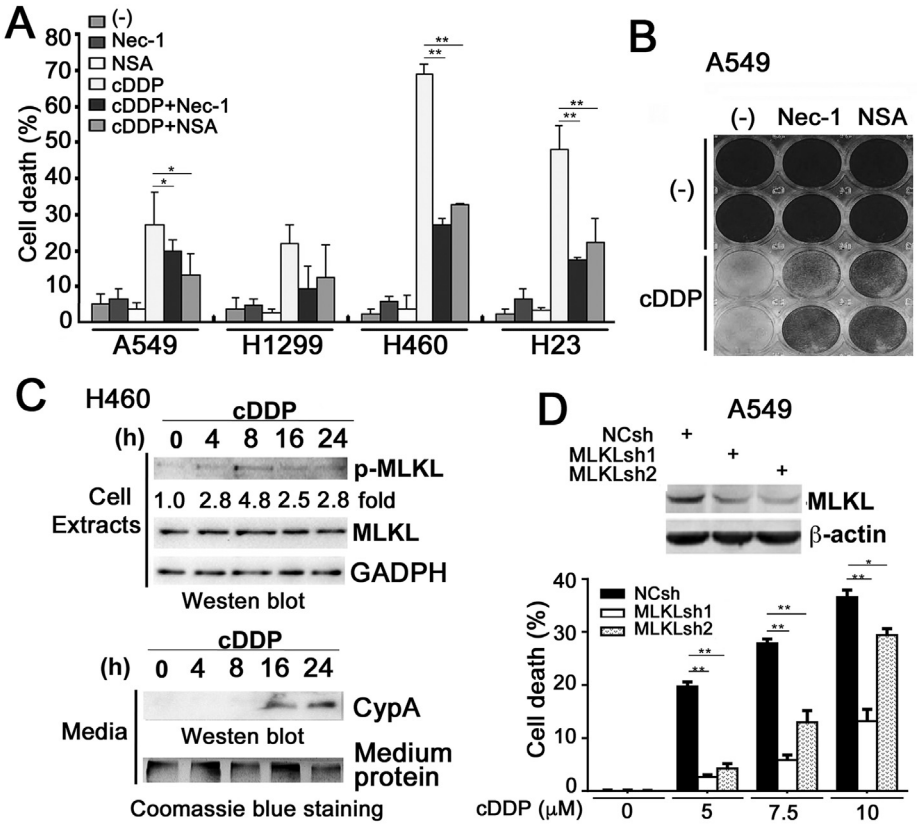

Figure 1. Cisplatin induces necroptosis in NSCLC cells. A. The cells were treated with Necrostatin-1 (Nec-1, 10 μM) or NSA (5 μM) for 30 min or remained untreated, and then with cisplatin (cDDP, 10 μM) for 48 hours and cell death was detected by LDH release assay. B. A549 cells were treated with Nec-1 (10 μM) or NSA (5 μM) plus cDDP (5 μM) for 2 days, then cultured in fresh medium for 10 days and stained with methylene blue. C. H460 cells were treated with cDDP (5 μM) for the indicated times. Top, the indicated proteins in cell lysates were detected by Western blot. GADPH was detected as an input control. Bottom, Cyclophilin A (CypA) in culture media was detected by Western blot. The major band detected in the gel by coomassie blue staining representing the major media protein was used as an input control. D. A549 cells were stably transfected with MLKL shRNA or negative control (NC) shRNA, MLKL knockdown was confirmed by Western blot (top). The cells were treated with cisplatin for 48 hours. Cell death was detected by LDH releasing assay. Data shown are the mean ± SD. *$P < 0.05$, **$P < 0.01$.

the dead cells displayed necrotic features such as rupture of cytoplasmic membrane, whereas retaining relatively normal nuclear morphology (Fig. S1A). When the cells were pretreated with necroptosis inhibitors necrostatin 1 (Nec-1) and NSA, cisplatin-induced cytotoxicity was substantially reduced, based on LDH release and clonogenic assays that reflect acute and chronic cytotoxicity, respectively (Figure 1*A* and *B*, S1C). Phosphorylation of the key necroptosis factor MLKL, a biomarker for necroptosis activation [9], and release of the necrosis marker of cyclophilin A to culture media, a necrotic cell death marker [35], were detected in cisplatin-treated cells (Figure 1*C*). Importantly, suppressing MLKL with RNAi effectively suppressed cytotoxicity induced by chemotherapeutics including cisplatin, vincristine, and adriamycin (Figure 1*D*, S1D-S1F). Altogether, these results support necroptosis as one important process in chemotherapy-induced cancer cell death.

RIP3 Expression is Suppressed in Human NSCLC

Immunohistochemistry (IHC) was used to detect expression of the key necroptosis factor, RIP3. A tissue array containing paired tumor and adjacent normal tissues from 45 NSCLC cases was stained for RIP3 protein and representative images are shown in Figure 2*A*. Decreased RIP3 expression in tumor compared with the corresponding adjacent normal tissue was detected in 12/45 (26.7%) NSCLC cases. When these samples are separated by the tumor histology, 24/45 (53.3%) were lung adenocarcinomas (LUAD) cases, whereas the remaining 21/45 (46.7%) were lung squamous cell carcinomas (LUSC) cases (Figure 2*B* top). The reduction in RIP3 expression was seen 8/24 (33.3%) LUAD and 4/21 (19.0%) LUSC tumors (Figure 2*B* top). These findings were validated using IHC staining of an independent sample set of surgically resected tumor–normal pairs from NSCLC 115 cases. Reduced RIP3 expression was seen in 27.0% (31/115) NSCLC tumors, including 23.4% (15/64) of LUAD and 31.4% (16/51) of LUSC tumors (Figure 2*B* bottom). While there was no statistical difference between clinicopathological features, including age, smoking history, stages, lymph rode metastasis and tumor size, and RIP3 protein expression (Table 1), reduced RIP3 expression was significantly associated ($P = 0.03$) with poorer chemotherapy response (Table 2). In addition, a trend of RIP3 mRNA expression reduction in lung cancer was detected in

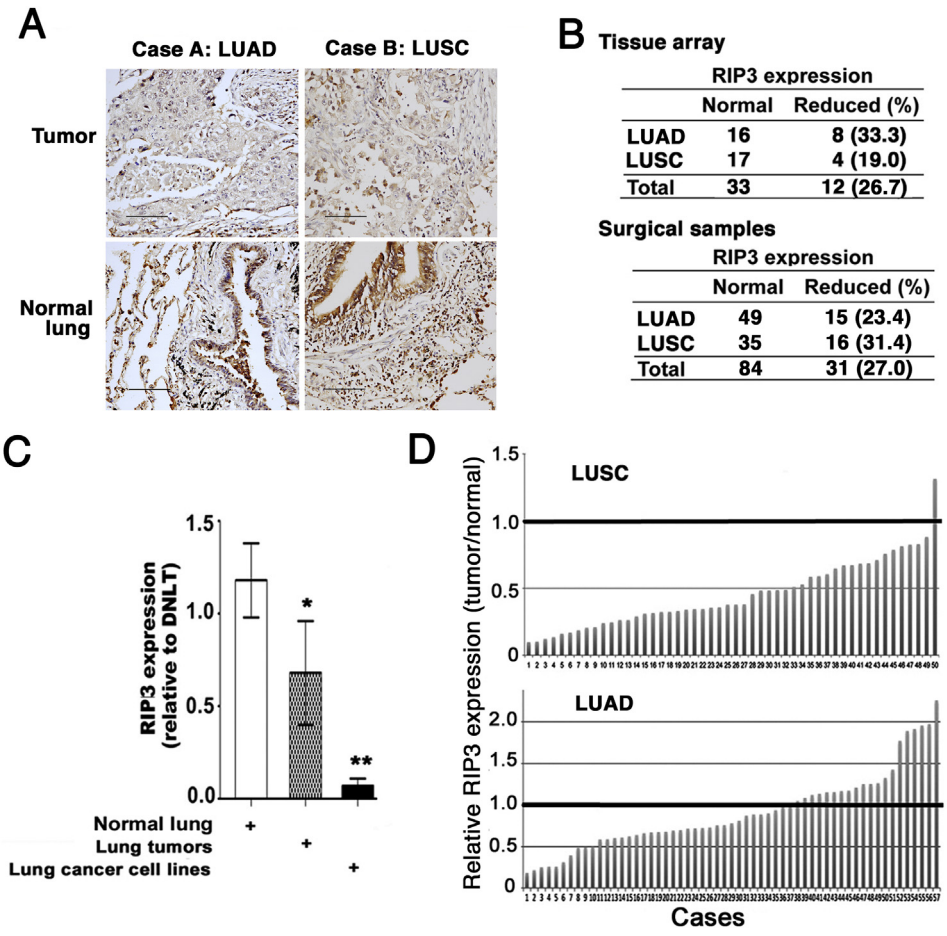

Figure 2. RIP3 expression is reduced in NSCLC. A. Human lung tumors with paired adjacent normal lung tissues in tissue arrays were stained for RIP3. Representative images (200×) are shown. Bar size: 100 μM. The airway and alveolar epithelial cells are strongly positive RIP3 in the adjacent tissues, whereas the tumor cells are weakly positive in the tumor tissues. B. Quantitative results derived from IHC of the tissue array (top) and surgical dissected samples (bottom). LUAD: Lung adenocarcinomas; LUSC: Lung squamous carcinomas. C. RIP3 mRNA expression quantified by qRT-PCR. Lung cancers are compared with paired normal lung ($n = 12$). Average of RIP3 expression in lung cancer cell lines are shown ($n = 14$). The RIP3 expression in distant normal lung tissue (DNLT) was used as a normal expression level for comparison. D. Data from MethHC was analyzed. The related RIP3 expression in tumor–normal pairs was shown. The tumor/normal ratios <1 means decreased RIP3 expression in tumors.

Table 1. Relationship Between Clinicopathological Features and RIP3 Protein Expression in Lung Cancer

Clinicopathological Features	Number ($n = 115$)	RIP3 Low	RIP3 High	*P* Value
Age				
<50	96	27	69	0.53
≤50	19	4	15	
Smoke				
Smoker	60	20	40	0.11
Nonsmoker	55	11	44	
Stage				
LUAD				
Stage I	13	1	12	0.80
Stage II	23	7	16	
Stage III	21	6	15	
Stage IV	7	1	6	
LUSC				
Stage I	25	8	17	0.39
Stage II	8	1	7	
Stage III	18	7	11	
Stage IV	0	0	0	
Tumor Size				
<2.0 cm	4	2	2	0.24
≥2.0 cm ≤ 5.0 cm	44	8	36	
≥5.0 cm	15	6	9	
Unknown	52	15	37	
Lymph Node Metastasis				
Positive	29	7	22	1.00
Negative	29	7	22	
Unknown	57	17	40	

tumor−normal pairs and NSCLC cell lines detected by qRT-PCR (Figure 2*C*). RIP3 mRNA expression reduction was more evident in cell lines than that in lung tumor tissues, which may be due to the more homogenous quality of the cancer cell lines (Figure 2*C*). The trend of reduced RIP3 mRNA expression in lung tumors was validated with an independent data set from an online resource (Figure 2*D*, MethHC, http://methhc.mbc.nctu.edu.tw/php/diffMeth.php). Supportively, RIP3 mRNA expression reduction was seen in 33 (77%) of the 43 NSCLC cell lines with available RNAseq data from the Broad Institue Cancer Cell Line Encyclopedia (CCLE, https://portals.broadinstitute.org/ccle/page?gene=RIPK3, Fig. S2). Consistently, RIP3 protein expression was reduced by 30~90% compared with the two immortalized human bronchial epithelial cell (HBEC) lines, detected by Western blot (Figure 3*A*). These results strongly suggest that RIP3 is suppressed in NSCLC.

Reduced RIP3 Expression in NSCLC is Associated With Promoter Methylation

The extent of cisplatin-induced cytotoxicity was correlated with expression levels of the key necroptosis mediator RIP3 (Figures 1*A* and 3*A*), and the reduction in RIP3 expression was seen both in protein (Figure 2*A*−*B*) and mRNA (Figure 2*C*−*D*, and S2) levels, suggesting that transcriptional suppression of RIP3 contributes to cisplatin-resistance. Because the promoter region of RIP3 is CpG rich and could be prone to abnormal DNA methylation, we evaluated its methylation status in human lung tumors and NSCLC cell lines using COBRA. Hypermethylation (detected by the digestion of RIP3 PCR products into smaller fragments following the addition of *BstUI* or *Taq I* enzymes) was detected in all the lung cancer cell lines but not in primary human bronchial epithelial cells (Figure 3*B*). Genome-wide methylation of lung tumor−normal pairs from an independent group of 16 NSCLC patients was also evaluated using the Human Methylation 450K (HM450) array (Illumina). The quantitative methylation data for five probes located within the promoter CpG island of RIP3 revealed significantly higher methylation in 4/16 (25%) tumors, the NSCLC cell line Calu-6, but not in primary human bronchial epithelial cells and normal lung tissues (Figure 3*C*). RIP3 mRNA and protein expression was partly restored after demethylation treatment with DAC and TSA in cancer cell lines having RIP3 promoter methylation (H23, H1568 and H2023), but not those having no promoter methylation (H1869 and HCC4006, Figure 3*D*), suggesting that promoter methylation underlies one of the main mechanisms for RIP3 suppression. By Western blot, RIP3 protein expression was increased after DAC and TSA treatment in A549 and H460 cells (Figure 3*E*). Notably, HeLa that has lost RIP3 expression exerted no signal, confirming the specificity of RIP3 antibody (Figure 3*E*). These findings corroborate a previous report showing RIP3 promoter methylation in 20% (3/15) of NSCLC [36], and

Table 2. Chemotherapy Response and RIP3 Protein Expression in NSCLC

Chemotherapy Response	*Number (n = 25)*	*RIP3 Reduced*	*RIP3 High*	*P Value*
Responded	11	3	8	
No Response	14	10	4	
% Responders	44%	23.1%	66.7%	0.03

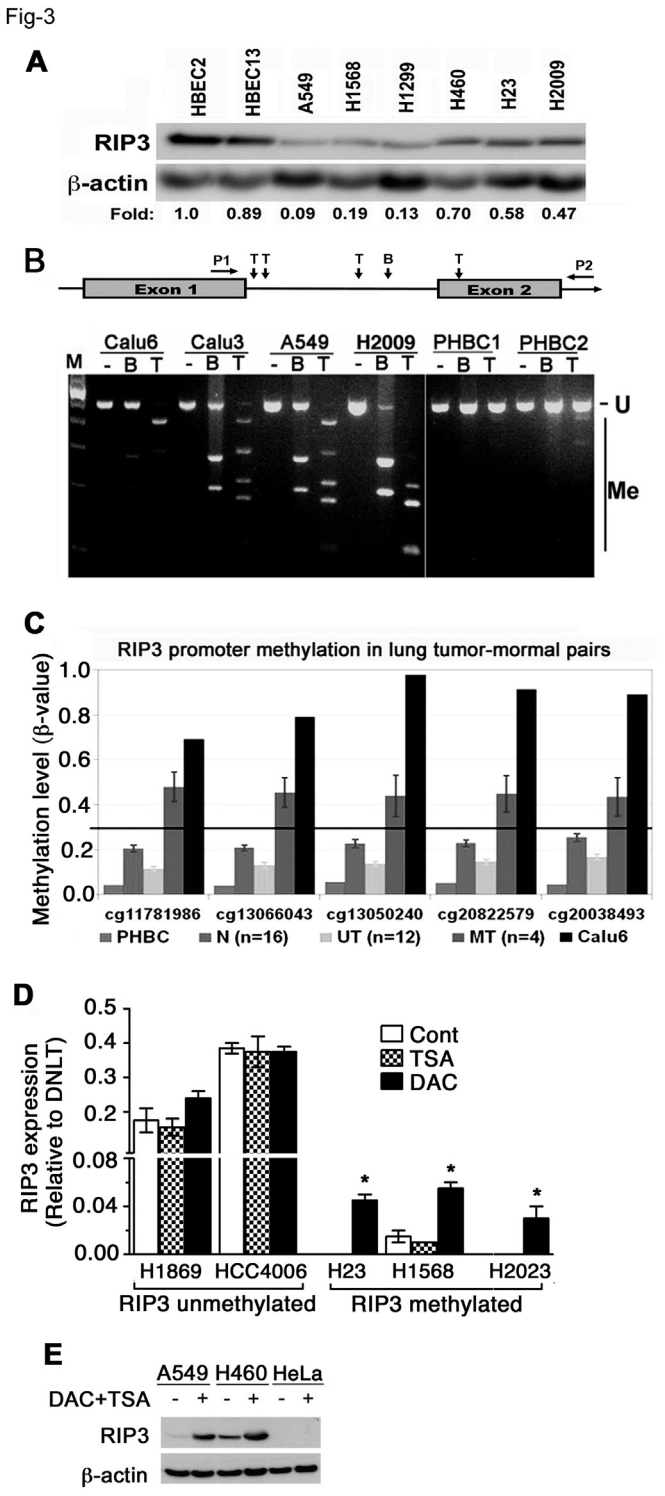

Figure 3. Reduced RIP3 expression associated with RIP3 promoter methylation in human NSCLC. A. RIP3 was detected in nontransformed (HBEC-2, -13) and lung cancer cell lines by Western blot. β-actin was detected as an input control. Relative RIP3 expression fold (HBEC-2 was set as 1) is shown at the bottom. B. *Upper,* A diagram of RIP3 promoter structure with the location of the primer and restriction sites analyzed by COBRA is shown. B, *BSTUI*, T, *Taq* I. *Lower,* NSCLC lines and primary human bronchial epithelial cells (PHBC1 and 2) were analyzed by COBRA using the restriction enzymes *BSTUI* (B) or *Taq* I (T) for digesting the RIP3 promoter PCR products. C. Quantitative analysis of RIP3 methylation. Genome-wide methylation of PHBC derived from a cancer free individual, lung tumor–normal pairs from 16 NSCLC patients, and the Calu6 NSCLC cells were evaluated with the Illumina HM450 Beadchip. Methylation level measured in β-values ranges from 0 to 1 and indicate 0–100% methylation, respectively. Five probes located within the RIP3 promoter CpG island were analyzed and $\beta \geq 0.3$ were considered methylated. Out of 16, 4 (25%) tumors, but not PHBC and normal lung tissues (0/16, 0%), show methylation of all five probes. N: normal tissue, UT: unmethylated tumor, MT: methylated tumor. D. The cell lines were treated with 1 μM 5-aza-2′-deoxycytidine (DAC) every 24 hours for 96 hours and/or 300 nM Trichostatin A (TSA) for 18 hours, and RIP3 mRNA expression was detected by qRT-PCR. $^{*}P < 0.05$; $^{**}P < 0.01$. E. The cells were treated as described in D, and RIP3 protein expression was detected by Western blot. β-actin was detected as an input control.

suggest that promoter methylation is partly responsible for RIP3 suppression in lung cancer.

Ectopic RIP3 Expression Restores Necroptosis and Sensitizes NSCLC Cells to Chemotherapy

The observation that the extent of cisplatin-induced cytotoxicity was correlated to RIP3 expression levels (Figures 1*A* and 3*A*) suggested that RIP3 expression is one of the necroptosis determinants, and its reduction in lung cancer cells may attenuate necroptosis. Thus, we restored RIP3 expression by stable transfection in A549 cells that have relatively low RIP3 protein (Figure 4*A*). Ectopic RIP3 expression strongly restored the necroptosis pathway, as shown by substantial augmentation of cell death induced by TNFα/z-VAD/Smac mimic that was blocked by necrostatin-1 (Fig. S1B) [37]. Then, the effect of ectopic RIP3 expression on cisplatin-induced cell death was examined. Restoration of RIP3 expression sensitized cells to cisplatin-induced cytotoxicity (Figure 4*B* and *C*, S1C), whereby the dead cells showed a necrotic morphology (Fig. S1A). The RIP3 expression potentiated cell death was effectively suppressed by necrostatin-1 or NSA (Figure 4*D*), consistent with the role of RIP3 in necroptosis. To validate the results, RIP3 was knocked down in H2009 cells that have relatively high RIP3 expression (Figures 3*A* and 4*E*), and the effect on cisplatin-induced cell death was examined. RIP3 knockdown effectively reduced cisplatin-induced cytotoxicity in H2009 cells (Figure 4*F*). These results support RIP3 expression contributes to suppression of the necroptosis pathway in lung cancer cells.

Restoration of RIP3 Expression Sensitizes Chemotherapeutic Drug Response In vivo

The effect of restoration of RIP3 expression on chemotherapy response was validated with a nude mouse xenograft therapy model in vivo. A549 cells with or without ectopic RIP3 expression (RIP3 or NC) were injected subcutaneously into nude mouse for the development of xenograft tumors followed by cisplatin therapy. Consistent with the in vitro results, cisplatin more profoundly retarded tumor growth in the RIP3 group (Figure 5*A*–*C*). The tumor inhibitory rate of cisplatin in the RIP3 group (75%) was higher than that in the NC group (55%, Figure 5*D*). Interestingly, while cisplatin induced both apoptotic (positive for both TUNEL and active caspase-3) and necrotic death (TUNEL-positive but active caspase-3-negative) in tumor tissues derived from NC cells, it mainly increased necrotic death in the RIP3 group (Figure 5*E*–*F*). These

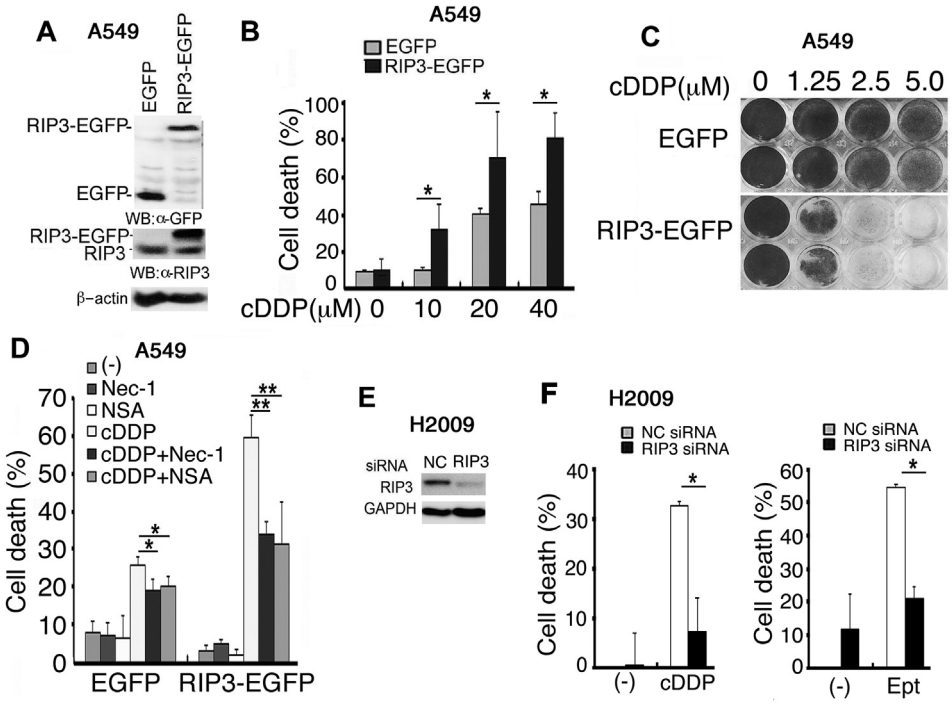

Figure 4. Ectopic RIP3 expression sensitizes cisplatin-induced cytotoxicity. A. Stable transfection of RIP3-EGFP or negative control EGFP vector in A549 cells. The expression of ectopic RIP3-EGFP was confirmed by Western blot. B. The cells were treated with cisplatin (cDDP) for 48 hours and cell death was detected by LDH release assay. *$P < 0.05$. C. The cells were treated with indicated concentrations of cDDP for 2 days, then cultured in fresh medium for 10 days and stained with methylene blue. D. The cells were treated with Nec-1 (10 μM) or NSA (5 μM) plus cisplatin for 48 hours, and cell death was detected by LDH release assay. E. The cells were transfected with RIP3- or negative control (NC)-siRNA. RIP3 knockdown was confirmed by Western blot. F. The cells were treated with for 30 min or remained untreated, and then with cisplatin (cDDP, 30 μM) or etooside (Ept, 20 μM) for 48 hours and cell death was detected by LDH release assay. *$P < 0.05$, **$P < 0.01$.

results support that restoration of RIP3 expression sensitizes cisplatin response mainly through potentiation of necroptosis.

RIP3 Expression Levels are Associated with Response to Platinum-based Chemotherapy in NSCLC Patients

Among the NSCLC cases whose surgical samples were examined for RIP3 protein expression (Figure 2*B*), 25 received platinum-based chemotherapy. These cases were chosen to compare the relationship between RIP3 expression of the tumor sample and the patient response to chemotherapy. Response to therapy was examined by CT scan, and patients with complete or partial tumor regression or stable disease were regarded as chemotherapy responders. The response rate among 13 cases whose tumors showed reduced RIP3 expression was 23.1% (3/13), which was significantly lower compared with patients with high RIP3 expression tumors (66.7%, 8/12, $P = 0.03$, Table 2). These results are consistent with a recent report showing that a higher RIP3 expression was associated with a better outcome of cisplatin--based adjuvant chemotherapy in patients after lung adenocarcinoma resection [38].

Discussion

This study provides evidence substantiating the role of necroptosis in anticancer chemotherapy. Although chemotherapeutic drugs trigger necroptosis in human lung cancer cells, this cell death pathway is suppressed in a subset of NSCLC. Our data show that the suppression of necroptosis could be attributed to RIP3 suppression, because 1) RIP3 expression in lung cancer is significantly decreased, 2) restoration of RIP3 expression strongly sensitized lung cancer cells to the cytotoxic effect of anticancer drugs, and 3) this sensitization can be suppressed by necroptosis inhibitors. RIP3 suppression was associated with RIP3 promoter methylation, and demethylation partly restored RIP3 expression and potentiated cytotoxicity induced by chemotherapy. In a xenograft tumor therapy model, ectopic RIP3 expression significantly sensitized anticancer activity of cisplatin in vivo. The clinical significance of these findings is supported by the fact that reduced RIP3 expression is associated with worse response in NSCLC patients receiving chemotherapy. Thus, the necroptosis pathway is suppressed in NSCLC, at least partly through RIP3 promoter methylation, and reactivating this pathway could be exploited for improving chemotherapy efficacy.

Although the molecular mechanisms by which chemotherapy suppresses cancer are diverse, ranging from DNA damage to cytoskeletal structure interruption, chemotherapeutics eventually induce cell death. Apoptosis is one of the cell death modes underlying the anticancer activity of chemotherapeutics, and acquired apoptosis resistance was frequently found in cancer with acquired chemoresistance [39–41]. However, chemoresistance still remains as a major clinical problem in spite of tremendous commitments in apoptosis resistance studies. Therefore, other cell death pathways could be involved in cancer cell's response to chemotherapy [42]. In this report, we determined that the chemotherapeutics including cisplatin, etoposide, and doxorubicin induce necroptosis, and the extent of cisplatin-induced cytotoxicity was well correlated to RIP3 expression

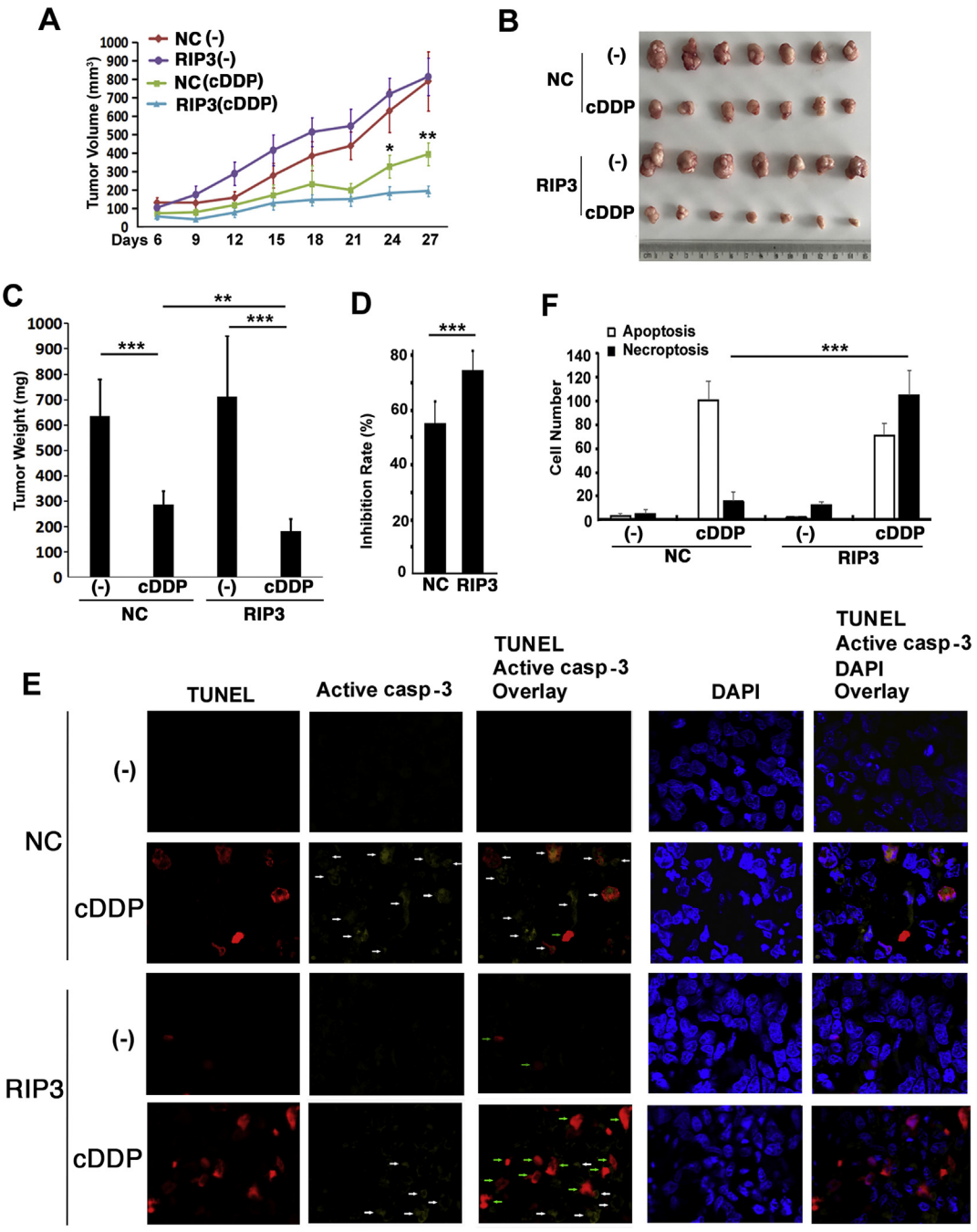

Figure 5. Restoration of RIP3 expression sensitizes cisplatin response in vivo. A. Tumor growth was measured every three days and the mean tumor volume of each group was shown. Comparison: NC (cDDP) vs RIP3 (cDDP); *, $p < 0.05$, **, $p < 0.01$. B. Resected xenograft tumors. C. Tumor weights and, D. Tumor inhibition rates were compared between treatment groups. E. Detection of apoptosis and necroptosis in tumor tissues by TUNEL assay combined with immunofluorescent staining of active caspase-3. Nucleus was stained with DAPI. Apoptosis (active caspase-3 and TUNEL positive) and necroptosis (TUNEL-positive but active caspase-3-negative) cells were quantified by counting in a total of 300 cells in five fields (200 ×). Representative images were shown. White arrows, active caspase-3 positive cells (yellow). Green arrows, TUNEL-positive cells (red). F. Average apoptotic cell numbers and necroptotic cell numbers were shown as mean ± SD. Columns represent mean in each group, bars represent SD. **, $P < 0.01$, ***, $P < 0.001$.

level. Thus, necroptosis suppression resulting from RIP3 silencing could be a new chemoresistance mechanism that can be exploited in NSCLC. This hypothesis was validated through in vitro cell culture and in vivo xenograft tumor therapy studies, in which ectopic RIP3 expression significantly sensitized anticancer activity of cisplatin that was mainly associated with increased necrotic cell death. The clinical relevance of RIP3 expression in chemotherapy was validated in NSCLC patients, in which reduced RIP3 expression was associated with worse chemotherapy response. Altogether, our data support that the necroptosis pathway is suppressed in lung cancer, and approaches sensitizing the necroptosis pathway would increase the efficacy of chemotherapeutics.

Our data also revealed abnormal methylation of RIP3 promoter in lung tumors and cancer cell lines but not in primary human bronchial epithelial cells and epigenetic RIP3 repression allows these cells to escape from necroptosis. These findings are consistent with previous reports showing RIP3 promoter methylation in NSCLC [36,43], and support that RIP3 suppression in lung cancer may at least partly be due to promoter hypermethylation. Indeed, demethylation treatment was able to restore RIP3 expression in RIP3 promoter hypermethylated cells, which also improved the anticancer activity of cisplatin in vitro. Therefore, our findings support that the necroptosis pathway in lung cancer is at least in part suppressed epigenetically, and approaches restoring RIP3 expression including via epigenetic therapy would increase the anticancer efficacy of chemotherapy.

It should be noted that our results do not exclude the possibility that necroptosis may still be suppressed in cancer cells without reduced RIP3 expression. This is because necroptosis can be regulated by different mechanisms such as post-translational modification of RIP3 as well as changes in the regulation of the core necroptosis signaling complex necrosome [44]. Necrosome can mediate either caspase-8-mediated apoptosis or RIP3-mediated necrosis, whereas cIAPs and cFLIP are the key factors for deciding to execute these cell death pathways. cIAPs mediate RIP1 ubiquitination and NF-κB activation, thereby inhibiting necrosome formation and death signaling [11]. When cIAPs are suppressed, caspase activity regulated by cFLIP in the necrosome will influence the cell death mode: either RIP3-dependent necroptosis or caspase-dependent apoptosis [10]. We have found that suppressing cIAPs leads to necrosome formation when cancer cells undergo necroptosis [23]. Whether these regulatory mechanisms are involved in chemoresistance deserve further studies.

Necrotic cell death initiates pro-inflammatory signaling by releasing cellular contents that ignite inflammatory cell infiltration and cytokine secretion. While excess and systemic inflammation may cause adverse effects on patients and chronic inflammation promotes carcinogenesis, moderate acute local inflammation at the tumor site may be beneficial because it elicits anticancer immunity [45]. A recently study clearly showed that intratumoral activation of necroptotsis through engineered RIPK1 and RIPK3 expression strongly potentiates antitumor immunity [46]. Thus, future studies are warranted to investigate the role of necroptosis-mediated inflammation and anticancer immunity during chemotherapy. In addition to being a therapeutic target, it will be interesting to investigate if RIP3 expression and promoter methylation could be biomarkers for predicting chemotherapy response.

Conflict of interest

The authors declare no conflict of interest.

Acknowledgements

The authors thank Dr. Francis Ka-Ming Chan, University of Massachusetts Medical School for providing the pEGFP-N1-RIP3 plasmid. Analysis of RIP3 mRNA expression in lung tumors was based on data generated by MethHC (http://methhc.mbc.nctu.edu.tw/php/diffMeth.php). Analysis of RIP3 mRNA expression in NSCLC cell lines was based on RNAseq data from the Broad Institue Cancer Cell Line Encyclopedia (CCLE, https://portals.broadinstitute.org/ccle/page?gene=RIPK3). This study was supported by grants 1R21CA193633, P30 CA11800 (NCI/NIH, USA), 81372377 (National Natural Science Foundation of China), and 2018HH0014 (R&D Program for International S&T Cooperation and Exchanges of Sichuan province, China).

Appendix A. Supplementary data

Supplementary data to this article can be found online at https://doi.org/10.1016/j.tranon.2019.11.011.

References

[1] Siegel RL, Miller KD and Jemal A (2018). Cancer statistics, 2018. *CA A Cancer J Clin* **68**, 7–30.
[2] Boloker G, Wang C and Zhang J (2018). Updated statistics of lung and bronchus cancer in United States (2018). *J Thorac Dis* **10**, 1158–1161.
[3] Seve P and Dumontet C (2005). Chemoresistance in non-small cell lung cancer. *Curr Med Chem Anti Cancer Agents* **5**, 73–88.
[4] Hanahan D and Weinberg RA (2011). Hallmarks of cancer: the next generation. *Cell* **144**, 646–674.
[5] Ghavami S, Hashemi M, Ande SR, Yeganeh B, Xiao W, Eshraghi M, Bus CJ, Kadkhoda K, Wiechec E and Halayko AJ, et al (2009). Apoptosis and cancer: mutations within caspase genes. *J Med Genet* **46**, 497–510.
[6] Ocker M and Hopfner M (2012). Apoptosis-modulating drugs for improved cancer therapy. *Eur Surg Res* **48**, 111–120.
[7] Long JS and Ryan KM (2012). New frontiers in promoting tumour cell death: targeting apoptosis, necroptosis and autophagy. *Oncogene* **31**, 5045–5060.
[8] Galluzzi L, Vanden Berghe T, Vanlangenakker N, Buettner S, Eisenberg T, Vandenabeele P, Madeo F and Kroemer G (2012). Programmed necrosis from molecules to health and disease. *Int Rev Cell Mol Biol* **289**, 1–35.
[9] Galluzzi L, Vitale I, Aaronson SA, Abrams JM, Adam D, Agostinis P, Alnemri ES, Altucci L, Amelio I and Andrews DW, et al (2018). Molecular mechanisms of cell death: recommendations of the nomenclature committee on cell death 2018. *Cell Death Differ* **25**, 486–541.
[10] Feoktistova M, Geserick P, Kellert B, Dimitrova DP, Langlais C, Hupe M, Cain K, MacFarlane M, Hacker G and Leverkus M (2011). cIAPs block Ripoptosome formation, a RIP1/caspase-8 containing intracellular cell death complex differentially regulated by cFLIP isoforms. *Mol Cell* **43**, 449–463.
[11] Tenev T, Bianchi K, Darding M, Broemer M, Langlais C, Wallberg F, Zachariou A, Lopez J, MacFarlane M and Cain K, et al (2011). The Ripoptosome, a signaling platform that assembles in response to genotoxic stress and loss of IAPs. *Mol Cell* **43**, 432–448.
[12] Imre G, Larisch S and Rajalingam K (2011). Ripoptosome: a novel IAP-regulated cell death-signalling platform. *J Mol Cell Biol* **3**, 324–326.
[13] Han J, Zhong CQ and Zhang DW (2011). Programmed necrosis: backup to and competitor with apoptosis in the immune system. *Nat Immunol* **12**, 1143–1149.
[14] Shan B, Pan H, Najafov A and Yuan J (2018). Necroptosis in development and diseases. *Genes Dev* **32**, 327–340.
[15] Florean C, Song S, Dicato M and Diederich M (2019). Redox biology of regulated cell death in cancer: a focus on necroptosis and ferroptosis. *Free Radic Biol Med* **134**, 177–189.
[16] Darding M and Meier P (2012). IAPs: guardians of RIPK1. *Cell Death Differ* **19**, 58–66.
[17] Kreuzaler P and Watson CJ (2012). Killing a cancer: what are the alternatives? *Nat Rev Cancer* **12**, 411–424.
[18] Meylan E and Tschopp J (2005). The RIP kinases: crucial integrators of cellular stress. *Trends Biochem Sci* **30**, 151–159.
[19] Newton K, Sun X and Dixit VM (2004). Kinase RIP3 is dispensable for normal NF-kappa Bs, signaling by the B-cell and T-cell receptors, tumor necrosis factor receptor 1, and Toll-like receptors 2 and 4. *Mol Cell Biol* **24**, 1464–1469.
[20] He S, Wang L, Miao L, Wang T, Du F, Zhao L and Wang X (2009). Receptor interacting protein kinase-3 determines cellular necrotic response to TNF-alpha. *Cell* **137**, 1100–1111.
[21] Cho YS, Challa S, Moquin D, Genga R, Ray TD, Guildford M and Chan FK (2009). Phosphorylation-driven assembly of the RIP1-RIP3 complex regulates programmed necrosis and virus-induced inflammation. *Cell* **137**, 1112–1123.

[22] Zhang DW, Zheng M, Zhao J, Li YY, Huang Z, Li Z and Han J (2011). Multiple death pathways in TNF-treated fibroblasts: RIP3- and RIP1-dependent and independent routes. *Cell Res* **21**, 368−371.
[23] He W, Wang Q, Srinivasan B, Xu J, Padilla MT, Li Z, Wang X, Liu Y, Gou X, Shen HM and Xing C, et al (2014). A JNK-mediated autophagy pathway that triggers c-IAP degradation and necroptosis for anticancer chemotherapy. *Oncogene* **33**, 3004−3013.
[24] Ramirez RD, Sheridan S, Girard L, Sato M, Kim Y, Pollack J, Peyton M, Zou Y, Kurie JM and Dimaio JM, et al (2004). Immortalization of human bronchial epithelial cells in the absence of viral oncoproteins. *Cancer Res* **64**, 9027−9034.
[25] Wang X, Chen W, Zeng W, Bai L, Tesfaigzi Y, Belinsky SA and Lin Y (2008). Akt-mediated eminent expression of c-FLIP and Mcl-1 confers acquired resistance to TRAIL-induced cytotoxicity to lung cancer cells. *Mol Cancer Ther* **7**, 1156−1163.
[26] Wang Q, Chen W, Xu X, Li B, He W, Padilla MT, Jang JH, Nyunoya T, Amin S, Wang X and Lin Y (2013). RIP1 potentiates BPDE-induced transformation in human bronchial epithelial cells through catalase-mediated suppression of excessive reactive oxygen species. *Carcinogenesis* **34**, 2119−2128.
[27] Chen W, Xu X, Bai L, Padilla MT, Gott KM, Leng S, Tellez CS, Wilder JA, Belinsky SA and Scott BR, et al (2012). Low-dose gamma-irradiation inhibits IL-6 secretion from human lung fibroblasts that promotes bronchial epithelial cell transformation by cigarette-smoke carcinogen. *Carcinogenesis* **33**, 1368−1374.
[28] Tessema M, Willink R, Do K, Yu YY, Yu W, Machida EO, Brock M, Van Neste L, Stidley CA and Baylin SB, et al (2008). Promoter methylation of genes in and around the candidate lung cancer susceptibility locus 6q23-25. *Cancer Res* **68**, 1707−1714.
[29] Tessema M, Yingling CM, Picchi MA, Wu G, Liu Y, Weissfeld JL, Siegfried JM, Tesfaigzi Y and Belinsky SA (2015). Epigenetic repression of CCDC37 and MAP1B links chronic obstructive pulmonary disease to lung cancer. *J Thorac Oncol* **10**, 1181−1188.
[30] Tessema M, Yingling CM, Snider AM, Do K, Juri DE, Picchi MA, Zhang X, Liu Y, Leng S and Tellez CS, et al (2014). GATA2 is epigenetically repressed in human and mouse lung tumors and is not requisite for survival of KRAS mutant lung cancer. *J Thorac Oncol* **9**, 784−793.
[31] Livak KJ and Schmittgen TD (2001). Analysis of relative gene expression data using real-time quantitative PCR and the 2(-Delta Delta C(T)) Method. *Methods* **25**, 402−408.
[32] Zhang J, Yang Y, He W and Sun L (2016). Necrosome core machinery: MLKL. *Cell Mol Life Sci* **73**, 2153−2163.
[33] Wang H, Sun L, Su L, Rizo J, Liu L, Wang LF, Wang FS and Wang X (2014). Mixed lineage kinase domain-like protein MLKL causes necrotic membrane disruption upon phosphorylation by RIP3. *Mol Cell* **54**, 133−146.
[34] He S, Huang S and Shen Z (2016). Biomarkers for the detection of necroptosis. *Cell Mol Life Sci* **73**, 2177−2181.
[35] Christofferson DE and Yuan J (2010). Cyclophilin A release as a biomarker of necrotic cell death. *Cell Death Differ* **17**, 1942−1943.
[36] Fukasawa M, Kimura M, Morita S, Matsubara K, Yamanaka S, Endo C, Sakurada A, Sato M, Kondo T and Horii A, et al (2006). Microarray analysis of promoter methylation in lung cancers. *J Hum Genet* **51**, 368−374.
[37] Laukens B, Jennewein C, Schenk B, Vanlangenakker N, Schier A, Cristofanon S, Zobel K, Deshayes K, Vucic D and Jeremias I, et al (2011). Smac mimetic bypasses apoptosis resistance in FADD- or caspase-8-deficient cells by priming for tumor necrosis factor alpha-induced necroptosis. *Neoplasia* **13**, 971−979.
[38] Chung JH, Yoon SH, Kang YJ, Kim YS, Son BS, Kwon RJ, Han JH and Kim DH (2019). Receptor-interacting protein kinase 3 as a predictive adjuvant chemotherapy marker after lung adenocarcinoma resection. *Ann Transl Med* **7**, 42.
[39] Chang A (2011). Chemotherapy, chemoresistance and the changing treatment landscape for NSCLC. *Lung Cancer* **71**, 3−10.
[40] Chen J, Emara N, Solomides C, Parekh H and Simpkins H (2010). Resistance to platinum-based chemotherapy in lung cancer cell lines. *Cancer Chemother Pharmacol* **66**, 1103−1111.
[41] Fulda S (2009). Tumor resistance to apoptosis. *Int J Cancer* **124**, 511−515.
[42] Fulda S (2018). Repurposing anticancer drugs for targeting necroptosis. *Cell Cycle 2018, 1−8.*
[43] Koo GB, Morgan MJ, Lee DG, Kim WJ, Yoon JH, Koo JS, Kim SI, Kim SJ, Son MK and Hong SS, et al (2015). Methylation-dependent loss of RIP3 expression in cancer represses programmed necrosis in response to chemotherapeutics. *Cell Res* **25**, 707−725.
[44] Feng S, Yang Y, Mei Y, Ma L, Zhu DE, Hoti N, Castanares M and Wu M (2007). Cleavage of RIP3 inactivates its caspase-independent apoptosis pathway by removal of kinase domain. *Cell Signal* **19**, 2056−2067.
[45] Shiao SL, Ganesan AP, Rugo HS and Coussens LM (2011). Immune microenvironments in solid tumors: new targets for therapy. *Genes Dev* **25**, 2559−2572.
[46] Snyder AG, Hubbard NW, Messmer MN, Kofman SB, Hagan CE, Orozco SL, Chiang K, Daniels BP, Baker D and Oberst A (2019 Jun 21). Intratumoral activation of the necroptotic pathway components RIPK1 and RIPK3 potentiates antitumor immunity. *Sci Immunol* **4**(36). pii: eaaw2004. https://doi.org/10.1126/sciimmunol.aaw2004.